Int J Clin Exp Med 2016;9(12):23019-23030
www.ijcem.com /ISSN:1940-5901/IJCEM0034304

*Original Article*

# Ursolic acid protects MC3T3-E1 cells against dexamethasone-mediated apoptosis, ROS generation and inflammation through activation of IGF-1

Jian Chen, Dengwei He, Qiaoping Li, Zhongwei Wu, Wenjun Huang, Ye Zhu

*Department of Orthopedics, 5th Affiliated Hospital, Lishui Central Hospital, Wenzhou Medical University, Lishui 323000, China*

Received June 23, 2016; Accepted August 15, 2016; Epub December 15, 2016; Published December 30, 2016

**Abstract:** Ursolic acid (UA), a pentacyclic triterpenoid found in a variety of plants, has attracted considerable attention because of its important biological and pharmacological activities. However, its effect on osteoclasts and mechanism of action require further investigation. In the current study, MC3T3-E1 cells were treated with dexamethasone (DEX), a well-known synthetic glucocorticoid, to establish a glucocorticoid-induced osteoporosis model. Our findings demonstrated that treatment of MC3T3-E1 cells with DEX significantly decreased cell proliferation and expression level of insulin-like growth factor 1 (IGF-1) in a dose-dependent manner. However, pretreatment of MC3T3-E1 cells with UA before exposure to DEX significantly attenuated DEX-induced apoptosis and ROS generation and secretions of TNF-α and IL-6. In addition, pretreatment with UA markedly reduced DEX-induced IGF-1 downregulation. Similar to the protective effect of UA, overexpression of IGF-1 depressed not only DEX-induced cytotoxicity, but also BMP2 downregulation and decreases in ratio of OPG/RANKL and Bax/Bcl-2. Taken together, the findings of the present study have demonstrated for the first time that UA protects MC3T3-E1 cells against DEX-induced apoptosis, oxidative stress and inflammation through activating IGF-1.

**Keywords:** Osteoporosis, osteoblasts, ursolic acid, IGF-1

## Introduction

Osteoporosis is one of bone diseases characterized by low bone mass and micro-architectural deterioration with consequent increase in bone fragility and susceptibility to fracture [1]. The imbalance between osteoblastic bone formation and osteoclastic bone resorption results in bone loss, leading to osteoporosis. After aging and sex steroid deficiency, the therapeutic use of glucocorticoids is the most common cause of osteoporosis [2]. They inhibit osteoblastogenesis and osteoclastogenesis and reduce osteoblast lifespan of through modifying the proliferative and metabolic activity of bone cells [3, 4]. Dexamethasone (DEX), a synthetic glucocorticoid, is well known to promote progenitor cells, such as bone marrow stromal cells, differentiates to the osteoblastic phenotype [5].

The processes of bone formation by osteoblasts and resorption by osteoclasts are regulated by multiple systemic and local factors, including GH, estrogen, insulin and insulin-like growth factor 1 (IGF-1) [6]. IGF-1 initiates cellular responses by binding to distinct cell-surface receptors that regulate a variety of signaling pathways controlling metabolism, growth and survival [7]. A reduction in IGF-I levels is implicated as an important factor in the etiology of evolutional osteoporosis, especially age-related bone loss [8]. In addition, it has been shown that IGF-1 treatment is effective in including gene expression of osteoblastic markers independent of age, indentifying exogenous IGF-1 as a potential beneficial treatment in age-related bone loss [9]. The IGF1 signaling abnormalities in osteoporotic osteoblasts were associated with reduced DNA synthesis both under basal conditions and after stimulation with

IGF1 [10, 11]. Whether abnormalities in IGF-1 signaling may explain altered IGF-1 action on human osteoblasts under specific conditions of net bone loss has not been determined.

Ursolic acid (UA) is a natural pentacyclic triterpenoid carboxylic acid, which is present in a various plants, including sea-weeds, fruits and many medicinal herbs, and thus their distribution is extensive in human diet [12, 13]. UA is known to have many important biological functions, including antitumor, anti-inflammatory, antioxidant, anti-hypertensive and anti-leukemic properties, combined with a low toxicity [14, 15]. The antitumor properties have been shown to be mediated by suppression of NF-κB activation and inhibiting the expression of COX-2, MMP9 and iNOS [16]. Furthermore, UA stimulated osteoblast differentiation *in vitro* and inducing new bone formation *in vivo* [17]. However, the mechanisms of its functions remain unclear.

In the present study, we investigated the cytoprotection of UA in MC3T3-E1 cells treated with DEX, a well-known synthetic glucocorticoid, which induces cell apoptosis, oxidative stress and inflammation [18]. Our findings showed that UA protected MC3T3-E1 cells against DEX-induced injury and inflammatory response by activating IGF-1.

## Materials and methods

### *Cell culture*

Murine preosteoblastic calvarial cells MC3T3-E1 was obtained from Shanghai Institute of Cell Biology (Shanghai, China). MC3T3-E1 cells were cultured in α-MEM medium (Hyclone, Logan, Utah, USA) supplemented with 10% fetal calf serum (Gibco, Rockville, MD, USA), 100 U/mL penicillin G (Solarbio, Beijing, China) and 100 μg/mL streptomycin (Solarbio) in a humidified atmosphere at 37°C with 5% $CO_2$.

### *Overexpression and construction of stable MC3T3-E1 cells*

Plasmid containing full length of IGF-1 was purchased from Sangon Biotech Co., Ltd. Full length of IGF-1 was amplified using PCR. The primers used were as follows: IGF-1-F, 5'-GCGAATTCATGACCGCACCTGCAATAAA-3' and IGF-1-R, 5'-CGGGATCCCTACTTGTGTTCTTCAAATG-3'. Then the PCR products were digested using *Eco*R I and *Bam*H I, and cloned into pCDNA3.1(+) (Addgene, Cambridge, MA, USA). The constructs were subsequently transfected into MC3T3-E1 cells using Lipofectamine 2000 (Invitrogen Life Technologies), according to the manufacturer's instructions. The black pCDNA3.1(+) was used as the negative control (NC).

### *Cell proliferation assay*

Cell proliferation was evaluated by Cell Counting Kit-8 (CCK-8, Dojindo, Kumamoto, Japan) assay as described previously [19]. In brief, MC3T3-E1 cells were seeded in 96-well plates at density of $3\times10^3$ cells/well and cultured in a humidified atmosphere at 37°C with 5% $CO_2$. When 80% confluence was reached, the cells were treated with conditioned medium as indicated. At 0, 24, 48 and 72 h, the culture supernatant was removed, and cells were washed with PBS, and then 100 μL of fresh medium mixed with CCK-8 solution was added to each well followed by a further 1 h incubation. The absorbance at wavelength 450 nm was measured for the supernatant of each well using a microplate reader (Shanghai Utrao Medical Instrument Co., Ltd., Shanghai, China).

### *Alkaline phosphatase activity assay*

The induction of alkaline phosphatase (ALP) is an unequivocal marker for bone cell differentiation. MC3T3-E1 cells were plated in 6-well plates at density of $5\times10^4$ cells/well and cultured in a humidified atmosphere at 37°C with 5% $CO_2$. After the cells were treated as indicated, the ALP activity in the supernatant was measured according to the previously described method [20]. Ultraviolet absorbance of the samples and standards were measured at 520 nm. Total protein was assayed by the method of Bradford [21].

### *Cell apoptosis assay*

Apoptosis was determined by flow cytometry analysis. MC3T3-E1 cells were plated in 6-well plates at density of $5\times10^4$ cells/well and cultured in a humidified atmosphere at 37°C with 5% $CO_2$. After the cells were treated as indicated, annexin-V fluorescein isothiocyanate (FITC)/propidium iodide (PI) double stain assays (BiovisionInc, Mountain View, CA, USA) were

performed following the manufacturer's protocol. Both floating and trypsinized adherent cells were collected, resuspended in 200 μL of binding buffer containing 195 μL of annexin-V FITC and 5 μL of propidium iodide (PI), and then incubated for 10 min in the dark at room temperature before flow cytometry analysis (BD Biosciences, Franklin Lakes, NJ, USA).

*Measurement of reactive oxygen species*

Reactive oxygen species (ROS) content was determined by fluorescent probe dichlorofluorescein diacetate (DCFH-DA) followed by flow cytometry. MC3T3-E1 cells were plated in 6-well plates at density of $5\times10^4$ cells/well and cultured in a humidified atmosphere at 37°C with 5% $CO_2$. After the cells were treated as indicated, 10 μM DCFH-DA was added following the manufacturer's protocol, and fluorescence intensity was measured using flow cytometry.

*Enzyme linked immunosorbent assay*

Secretions of TNF-α and IL-6 were determined by Enzyme linked immunosorbent (Elisa) assay kit (JRDUN Biotechnology Co., Ltd, Shanghai, China). MC3T3-E1 cells were plated in 6-well plates at density of $5\times10^4$ cells/well and cultured in a humidified atmosphere at 37°C with 5% $CO_2$. After the cells were treated as indicated, the relative content of each secreted inflammatory factors in the supernatant was measured by Elisa according to the manufacturer's protocol.

*Real-time PCR assay*

Total RNA was extracted using TRIzol reagent (Invitrogen Life Technologies, Carlsbad, CA, USA), according to the manufacturer's instructions. The complementary DNA was synthesized using a cDNA synthesis kit (Thermo Fisher Scientific, Rockford, IL, USA). Real-time PCR assay was performed using DyNAmo Flash SYBR Green kit (Finnzymes Oy, Espoo, Finland), and data collection was conducted using an ABI 7500 (Thermo Fisher Scientific). Sequences for the primers are as follows: IGF-1, forward: 5'-GAAATGAGTGGCTTCCCTTG-3' and reverse: 5'-GTTTACACAGCAGGTCAGAG-3'; GAPDH, forward: 5'-ATCACTGCCACCCAGAAG-3' and reverse: 5'-TCCACGACGGACACATTG-3'. GAPDH was used an internal control for normalization. The gene expression was calculated using the $2^{-\Delta\Delta Ct}$ method [22].

*Western blot assay*

Total protein was extracted from MC3T3-E1 cells using radioimmunoprecipitation buffer. The protein concentration was assessed using a bicinchoninic acid protein assay kit (Thermo Fisher Scientific). 25 μg protein lysates was separated by 10-15% SDS-PAGE and transferred to polyvinylidene fluoride membranes (Sigma-Aldrich), followed by incubated with primary antibodies against IGF-1 (1:3000), BMP2 (1:1000), OPG (1:1000), RANKL (1:1000), Bax (1:400), Bcl-2 (1:400) and GAPDH (1:1500), respectively, and incubated with secondary antibody labeled with horseradish peroxidase (1:1000). The blots were developed using enhanced chemiluminescence and determined using Image J software (National Institutes of Health, Bethesda, MD, USA).

*Statistics*

All experiments were performed repeatedly in three times. The data are expressed as the mean ± SD, and samples were evaluated by the unpaired, two-tailed Student's t-test using GraphPad Prism 5 software (GraphPad Software, Inc., La Jolla, CA, USA). The limit of significance for all analyses was defined as a *P* value of 0.05.

## Results

*DEX inhibits proliferation and IGF-1 expression in MC3T3-E1 cells*

To investigate the effect of DEX on growth of MC3T3-E1 cells, cell proliferation and ALP activity were detected by CCK-8 assay and ALP activity assay kit, respectively. As shown in **Figure 1A**, exposure of MC3T3-E1 cells to DEX at concentrations ranging from 0.01 to 10 μM for 24, 48 and 72 h led to a decrease in cell proliferation compared with control cells, in a dose- and time-dependent manner. Furthermore, exposure of MC3T3-E1 cells to DEX at concentrations ranging from 0.1 to 10 μM for 48 h led to a decrease in ALP activity in a dose-dependent manner (**Figure 1B**). Next we measured IGF-1 expression in response to DEX. Exposure of MC3T3-E1 cells to DEX at concentrations ranging from 0.01 to 10 μM for 48 h,

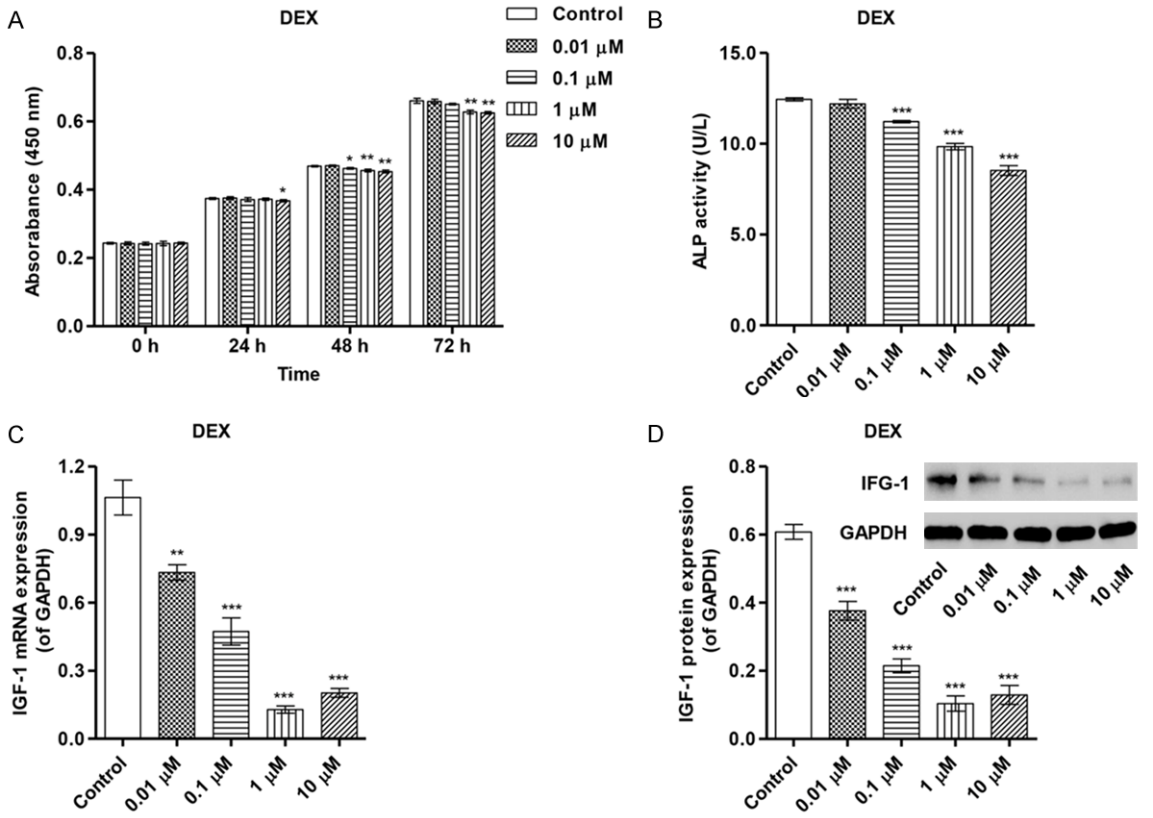


**Figure 1.** DEX inhibits proliferation and IGF-1 expression in MC3T3-E1 cells. (A) MC3T3-E1 cells were treated with DEX at concentrations of 0.01, 0.1, 1 and 10 μM for 0, 24, 48 and 72 h. Cell proliferation was measured by CCK-8 assay. (B) MC3T3-E1 cells were treated with DEX at concentrations of 0.01, 0.1, 1 and 10 μM for 48 h. ALP activity was measured at 520 nm with a microplate reader. MC3T3-E1 cells were treated with DEX at concentrations of 0.01, 0.1, 1 and 10 μM for 48 h. The expression of IGF-1 was measured by Real-time PCR (C) and Western blot assays (D). The intensity of the protein bands of a typical experiment was quantified with Image J 1.41 software. $^{*}P<0.05$, $^{**}P<0.01$, $^{***}P<0.001$ compared with control group.

the expression of IGF-1 was significantly decreased compare with control cells, at both mRNA and protein levels (**Figure 1C** and **1D**). These results suggest that DEX inhibits MC3T3-E1 cells proliferation may through decreasing the IGF-1 activity.

*UA inhibits DEX-induced cytotoxicity in MC3T3-E1 cells*

To investigate the effect of UA on DEX-induced cytotoxicity, cell proliferation and ALP activity were also measured. As shown in **Figure 2A**, treatment of MC3T3-E1 cells with UA at concentrations ranging from 0.1 to 1000 nM for 48 and 72 h led to an increase in cell proliferation compared with control cells, in a dose- and time-dependent manner (**Figure 2A**). Moreover, the decreased cell proliferation and ALP activity induced by 1 μM DEX treatment for 48 h was significantly inhibited by pretreatment with UA at 10, 100 and 1000 nM for 24 h, respectively (**Figure 2B** and **2C**). These findings indicate that UA pretreatment protects against DEX-induced toxicity in MC3T3-E1 cells.

*UA ameliorates DEX-induced apoptosis in MC3T3-E1 cells*

To elucidate whether the cytoprotection of UA was associated with its anti-apoptosis in DEX-induced MC3T3-E1 cells, the apoptotic rate was measured by flow cytometry. Exposure of MC3T3-E1 cells to 1 μM DEX for 48 h led to an increase in apoptotic rate (**Figure 3**). Prior to the Dex exposure, pretreatment with UA at 10, 100 and 1000 nM for 24 h significantly decreased apoptotic rate in DEX-induced MC3T3-E1 cells, indicating that DEX treatment impairs the endogenous antiapoptotic defense mechanism.

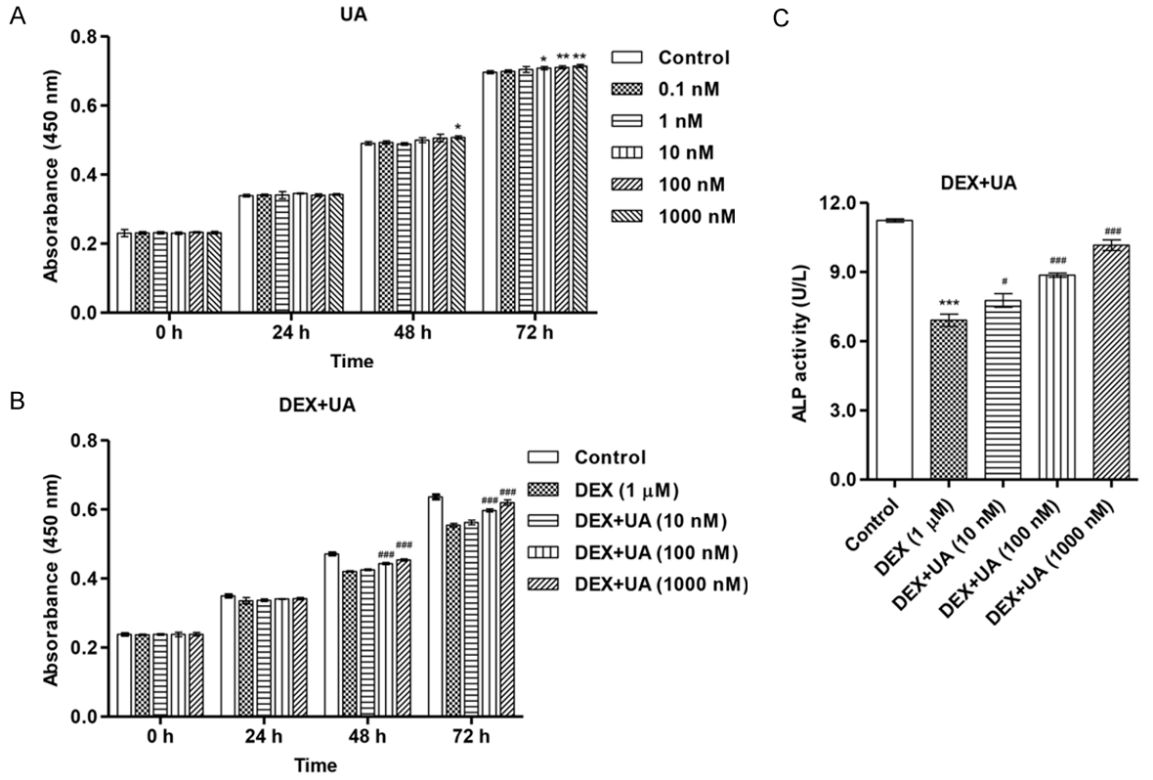


**Figure 2.** UA protects MC3T3-E1 cells against DEX-induced cytotoxicity. A: MC3T3-E1 cells were treated with UA at concentrations of 0.1, 1, 10, 100 and 1000 nM for 0, 24, 48 and 72 h. Cell proliferation was measured by CCK-8 assay. B: Before exposure to 1 μM DEX for 0, 24, 48 and 72 h, MC3T3-E1 cells were pretreated with different concentrations of UA for 24 h. Cell proliferation was measured by CCK-8 assay. C: Before exposure to 1 μM DEX for 0, 24, 48 and 72 h, MC3T3-E1 cells were pretreated with different concentrations of UA for 24 h. ALP activity was measured at 520 nm with a microplate reader. $^{*}P<0.05$, $^{**}P<0.01$, $^{***}P<0.001$ compared with control group. $^{\#}P<0.05$, $^{\#\#\#}P<0.001$ compared with DEX treatment group.

*UA represses DEX-induced ROS generation in MC3T3-E1 cells*

To elucidate whether the cytoprotection of UA was associated with its antioxidation in DEX-induced MC3T3-E1 cells, the intracellular ROS level was measured by flow cytometry. Treatment of MC3T3-E1 cells with 1 μM Dex for 48 h significantly increased intracellular ROS level (**Figure 4**). Importantly, pretreatment of UA at 10, 100 and 1000 nM for 24 h obviously attenuated the effect of DEX on intracellular ROS level in MC3T3-E1 cells. These findings suggest that the inhibition of cytotoxicity of UA is associated with its antioxidant effect.

*UA attenuates DEX-induced inflammatory factors secretions from MC3T3-E1 cells*

Next we measured TNF-α and IL-6 secretions in response to DEX and UA. After exposure of MC3T3-E1 cells to 1 μM DEX for 48 h, TNF-α and IL-6 secretions were significantly increased, respectively (**Figure 5A** and **5B**). Pretreatment with UA at 10, 100 and 1000 nM for 24 h before exposure to DEX markedly inhibited TNF-α and IL-6 secretions from MC3T3-E1 cells, respectively. These results indicate that UA possess an anti-inflammatory effect in DEX-induced MC3T3-E1 cells.

*Inhibition of IGF-1 downregulation contributes to the cytoprotection of UA in DEX-induced MC3T3-E1 cells*

After treatment of MC3T3-E1 cells with 1 μM DEX for 48 h, expression of IGF-1 was significantly decreased (**Figure 6A** and **6B**). Pretreatment with UA at 10, 100 and 1000 nM for 24 h markedly inhibited the downregulation of IGF-1 induced by DEX treatment. To investigate the role of IGF-1 in DEX-induced MC3T3-E1 cells, IGF-1 overexpression was constructed in MC3T3-E1 cells by transfected with

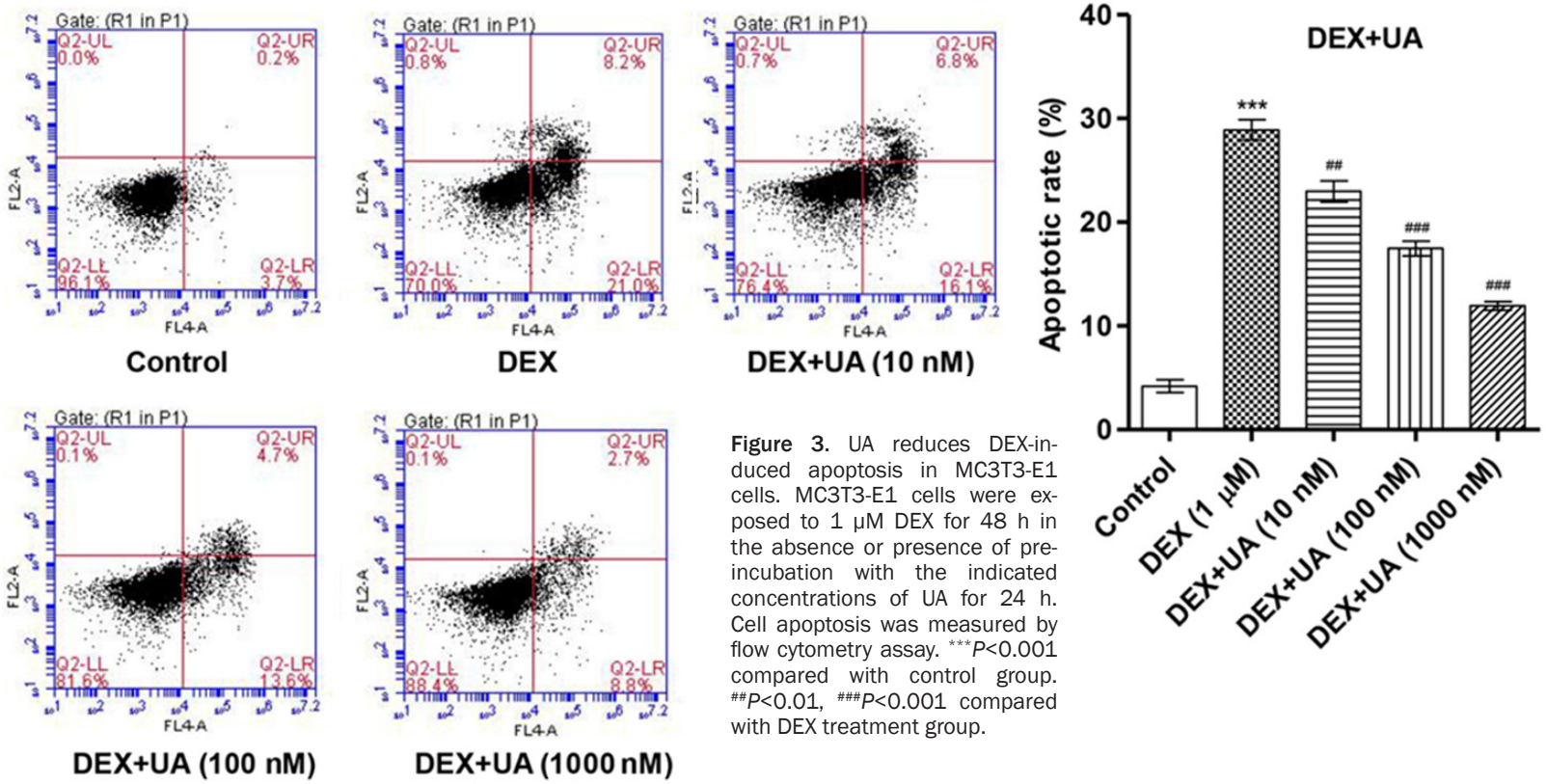


**Figure 3.** UA reduces DEX-induced apoptosis in MC3T3-E1 cells. MC3T3-E1 cells were exposed to 1 μM DEX for 48 h in the absence or presence of pre-incubation with the indicated concentrations of UA for 24 h. Cell apoptosis was measured by flow cytometry assay. $^{***}P<0.001$ compared with control group. $^{\#\#}P<0.01$, $^{\#\#\#}P<0.001$ compared with DEX treatment group.

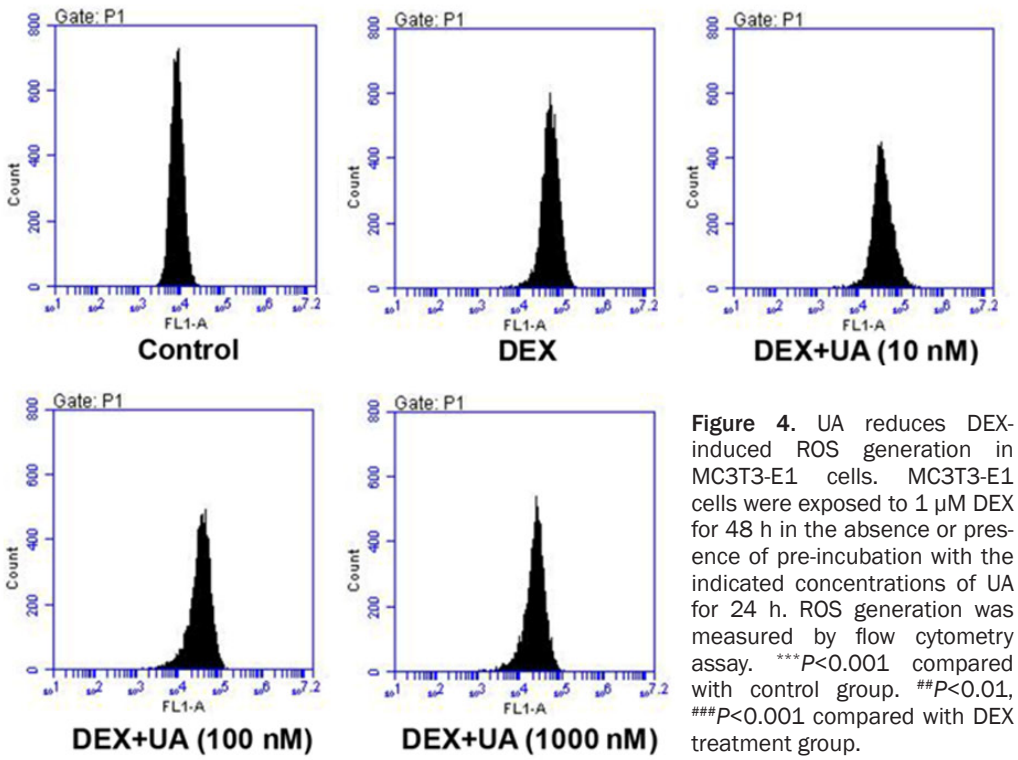


**Figure 4.** UA reduces DEX-induced ROS generation in MC3T3-E1 cells. MC3T3-E1 cells were exposed to 1 μM DEX for 48 h in the absence or presence of pre-incubation with the indicated concentrations of UA for 24 h. ROS generation was measured by flow cytometry assay. $^{***}P<0.001$ compared with control group. $^{\#\#}P<0.01$, $^{\#\#\#}P<0.001$ compared with DEX treatment group.

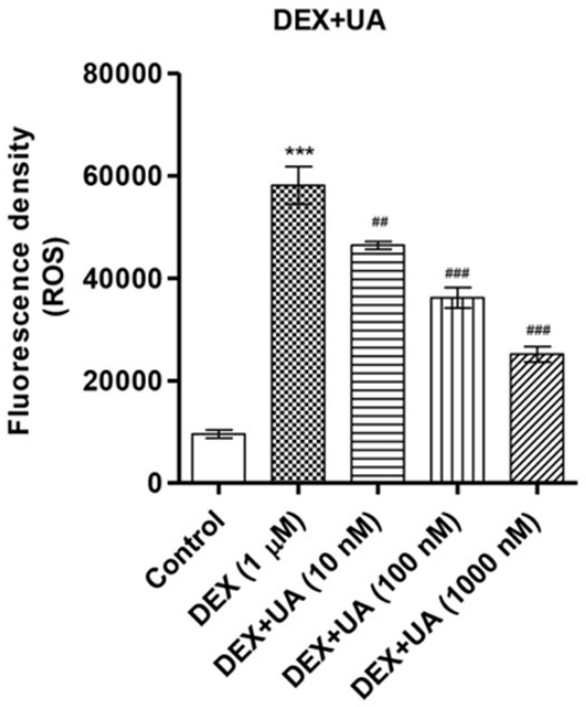

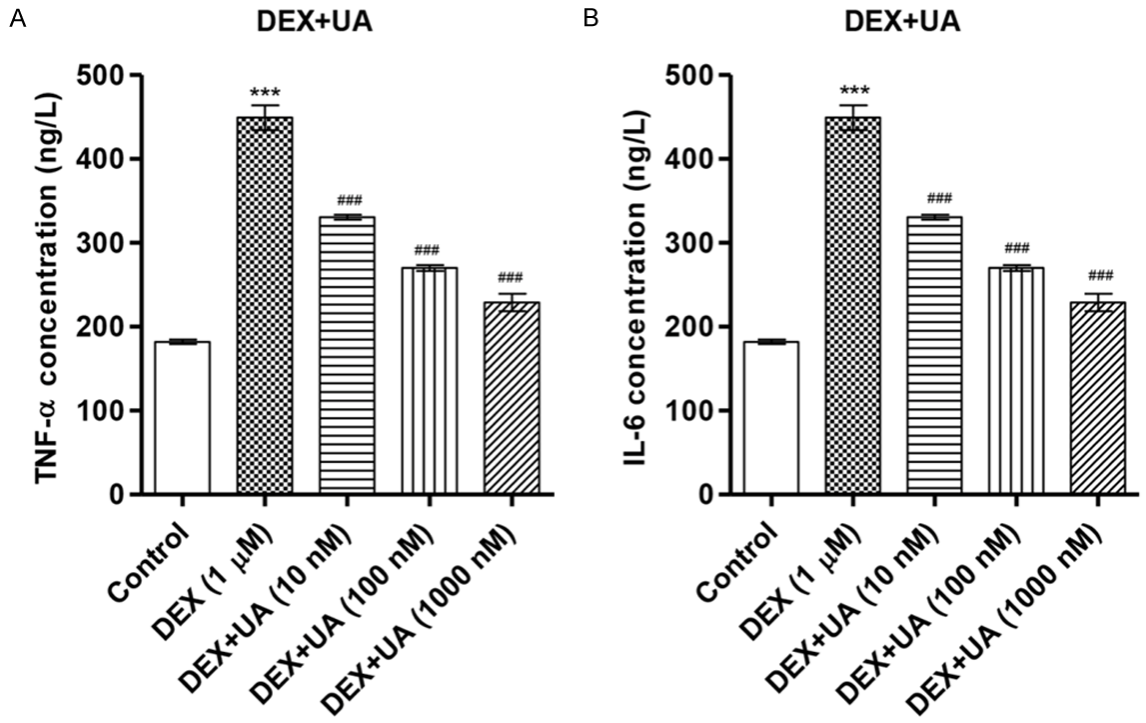


**Figure 5.** UA inhibits DEX-induced TNF-α and IL-6 secretions from MC3T3-E1 cells. MC3T3-E1 cells were exposed to 1 μM DEX for 48 h in the absence or presence of pre-incubation with the indicated concentrations of UA for 24 h. ELISA was performed to detect the levels of TNF-α (A) and IL-6 (B) in cell supernatants. $^{***}P<0.001$ compared with control group. $^{###}P<0.001$ compared with DEX treatment group.

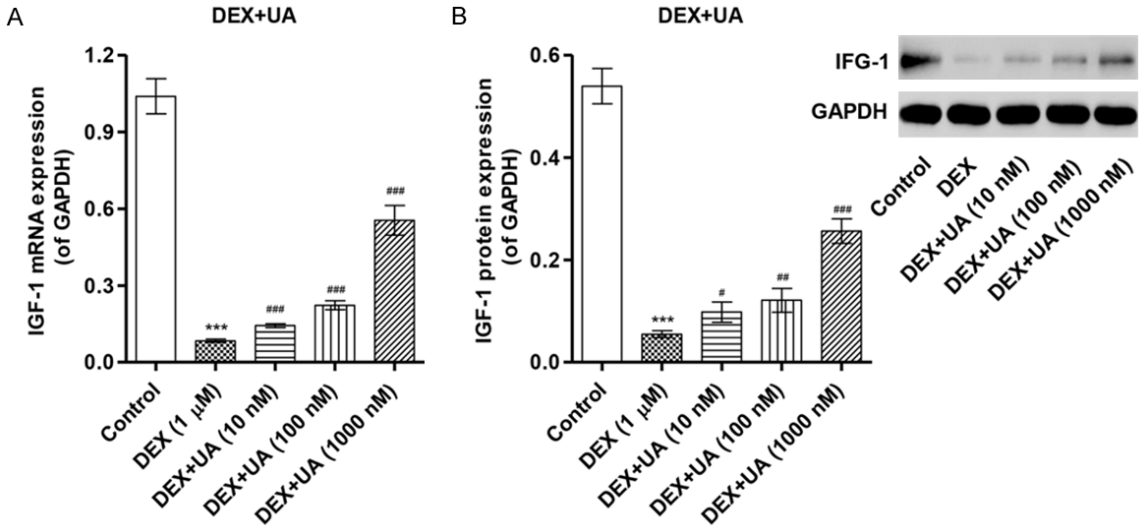


**Figure 6.** Effect of UA on DEX-induced IGF-1 downregulation. MC3T3-E1 cells were exposed to 1 μM DEX for 48 h in the absence or presence of pre-incubation with the indicated concentrations of UA for 24 h. The expression of IGF-1 was measured by Real-time PCR (A) and Western blot assays (B). The intensity of the protein bands of a typical experiment was quantified with Image J 1.41 software. ***P<0.001 compared with control group. #P<0.05, ##P<0.01, ###P<0.001 compared with DEX treatment group.

pCDNA3.1(+)-IGF-1. As shown in **Figure 7A** and **7B**, MC3T3-E1 cells transfected with pCDNA-3.1(+)-IGF-1 prior to DEX treatment for 48 h significantly increased the expression of IGF-1 at

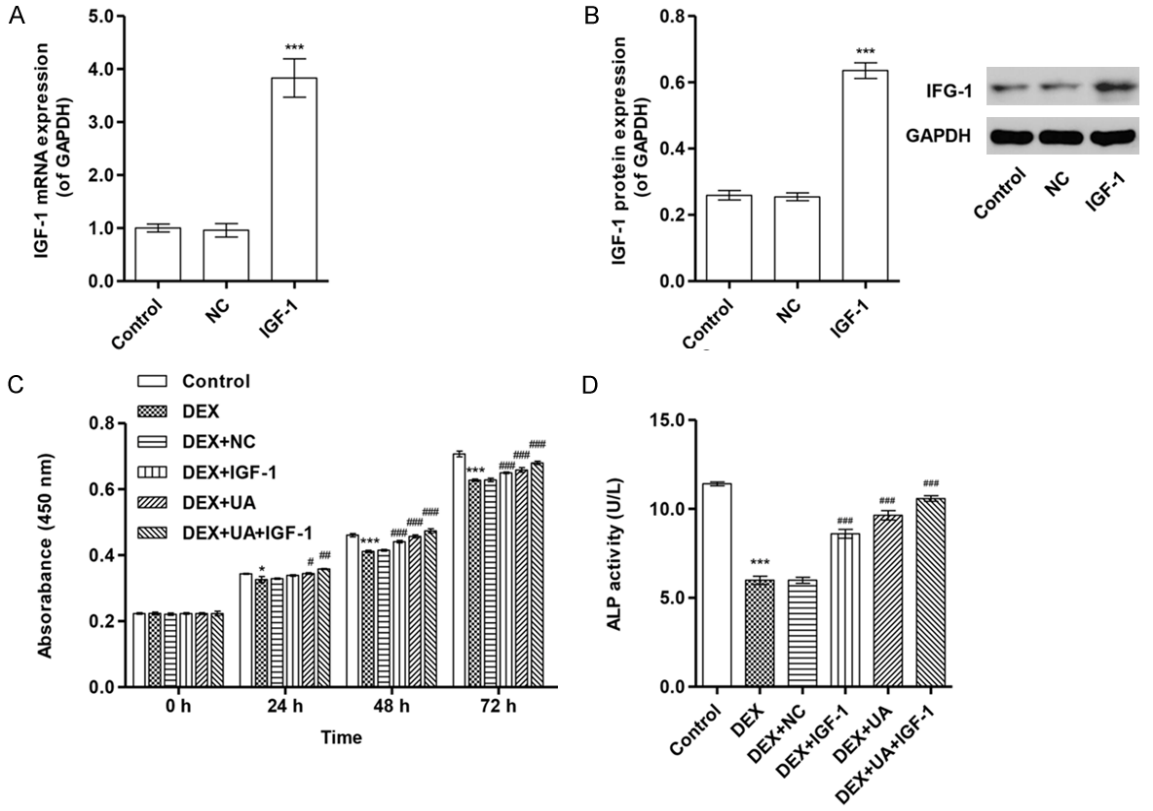


**Figure 7.** Effect of IGF-1 overexpression on proliferation and ALP activity of MC3T3-E1 cells. MC3T3-E1 cells were transfected with pCDNA3.1(+)-IGF-1 prior to 1 μM DEX treatment for 48 h. The expression of IGF-1 was measured by Real-time PCR (A) and Western blot assays (B). The intensity of the protein bands of a typical experiment was quantified with Image J 1.41 software. MC3T3-E1 cells were transfected with pCDNA3.1(+)-IGF-1 prior to 1 mM Dex treatment for 48 h in the absence or presence of pretreatment with UA at 100 nM for 24 h. (C) Cell viability was measured by CCK-8 assay. (D) ALP activity was measured at 520 nm with a microplate reader. $^{***}P<0.001$ compared with control group. $^{\#}P<0.05$, $^{\#\#}P<0.01$, $^{\#\#\#}P<0.001$ compared with DEX treatment group.

both mRNA and protein levels. IGF-1 overexpression could imitate the roles of UA in increase of proliferation and ALP activity (**Figure 7C** and **7D**). Importantly, treatment of DEX-induced MC3T3-E1 cells with both IGF-1 overexpression and 100 nM UA showed augmented effects on cell proliferation and ALP activity compared with DEX-induced MC3T3-E1 cells treated with IGF-1 overexpression or UA alone. These results suggest that IGF-1 mediated DEX-induced cytotoxicity, and that the inhibition of DEX-induced IGF-1 downregulation is involved in the UA-triggered protective effect in MC3T3-E1 cells.

*Effects of IGF-1 overexpression on protein expression in MC3T3-E1 cells*

To clarify the molecular mechanism of MC3T3-E1 cells proliferation inhibition and apoptosis induced by DEX, the expressions of related proteins were detected by Western blot. As shown in **Figure 8A-C**, treatment with 1 μM DEX for 48 h decreased BMP2 expression and OPG/RANKL ratio, whereas MC3T3-E1 cells with IGF-1 overexpression significantly reversed the effects of DEX on BMP2 expression and OPG/RANKL ratio. In addition, treatment with 1 μM DEX for 48 h decreased Bcl-2/Bax ratio, whereas MC3T3-E1 cells with IGF-1 overexpression significantly reversed the effects of DEX on Bcl-2/Bax ratio (**Figure 8A** and **8D**). Importantly, treatment of DEX-induced MC3T3-E1 cells with both IGF-1 overexpression and 100 nM UA showed augmented effects on these protein alternations compared with DEX-induced MC3T3-E1 cells treated with IGF-1 overexpression or UA alone.

## Discussion

Glucocorticoids have been known to be the most frequently used anti-inflammatory and

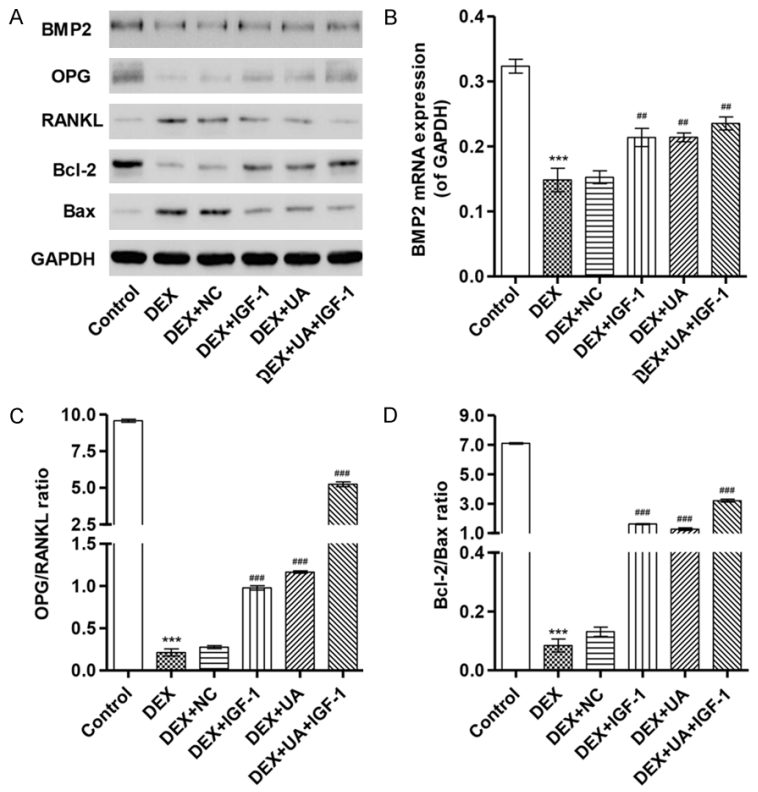


**Figure 8.** Effect of IGF-1 overexpression on protein expression in MC3T3-E1 cells. MC3T3-E1 cells were transfected with pCDNA3.1(+)-IGF-1 prior to 1 μM DEX treatment for 48 h in the absence or presence of pretreatment with UA at 100 nM for 24 h. The protein expression was measured by Western blot assay. (A) Cell lysates were subjected to Western blot analysis using BMP2, OPG, RANKL, Bcl-2 and Bax-specific antibody. The intensity of the protein bands of BMP-2 (B) OPG/RANKL (C) and Bcl-2/Bax (D) was quantified with Image J 1.41 software. $^{***}P<0.001$ compared with control group. $^{\#\#}P<0.01$, $^{\#\#\#}P<0.001$ compared with DEX treatment group.

immunosuppressive drugs in clinic to treat a variety of diseases, including inflammation, cancer and autoimmune disorders [23]. However, it has been found that continuous glucocorticoids treatment results in osteoporosis through affecting bone metabolism and induce apoptosis in osteoblasts, osteocytes, and numerous lymphoid tissues [24, 25]. Although the effects of glucocorticoids in bone remodeling have been reported, the mechanism of glucocorticoids involved in apoptosis, oxidative stress and inflammation of osteoblast is still poorly understood. Thus, to clarify the apoptotic mechanism of glucocorticoids in osteoblast, we used relatively high dose of DEX as an apoptotic inducer in MC3T3-E1 cells.

Our results showed that exposure of MC3T3-E1 cells to DEX led to cytotoxicity, evidenced by the decreased cell proliferation and ALP activity, and increased cell apoptosis. The inhibiting effects of DEX on cell proliferation and ALP activity increase in a dose-time dependent manner. ALP activity is considered to be an early marker of osteogenic differentiation, which is characterized by increased osteocalcin. In agreement with our findings, previous studies have been reported that DEX significantly reduced MC3T3-E1 cells viability and increased apoptosis in dose-dependent manner [26]. To investigate whether UA can protect MC3T3-E1 cells against DEX-induced cytotoxicity, MC3T3-E1 cells were pretreated with UA at concentrations ranging from 0.1 to 1000 nM for 24 h before exposure to DEX. Interestingly, we found that pretreatment with UA significantly attenuated DEX-induced cytotoxicity in MC3T3-E1 cells. This anti-cytotoxic effect of UA is similar to previous results in leukemic cells [27] and human lymphocytes [28].

Another important finding of this study was that UA inhibited oxidative stress and inflammatory response induced by DEX in MC3T3-E1 cells. UA protects against chronic ethanol-induced oxidative stress in the rat heart [29] and attenuates oxidative damage induced by D-galactose [30]. Additionally, UA exhibitsanti-inflammatory effects in RAW264.7 cells by attenuating iNOSand COX-2 expression [16]. In this study, UA inhibited DEX-induced increases in secretions of TNF-α and IL-6 inflammatory factors. Similarly, pro-inflammatory cytokines, such as IL-1α, TNF-α and IL-17 exhibit osteoclastogenic properties and some of them, such as IL-6, may produce both stimulating and suppressing actions on osteoclasts [31].

IGF-1 is a cytokine that plays an important role in the pathogenesis of osteoporosis by regulat-

ing growth and development [32]. Lower levels of serum IGF-1 appear to increase the risk of osteoporotic fractures in postmenopausal women and this may reflect a reduction in bone formation as demonstrated [33]. We found that DEX significantly decreased IGF-1 expression in a dose-dependent manner. However, UA corrected DEX-induced decrease in IGF-1 expression. Importantly, overexpression of IGF-1 in MC3T3-E1 cells possessed a similar effect of UA on cell proliferation, evidenced by increases in ALP activity, BMP2 expression and OPG/RANKL ratio, and apoptosis, evidenced by increased Bcl-2/Bax ratio. Previous study reported that DEX provokes bone resorption by increasing the synthesis of RANKL and inhibiting BMP2 and OPG production with consequent induction of osteoclastogenesis [34]. And the similar IGF-1 induced Bcl-2/Bax-dependent apoptotic pathway was also found in the previous study [35]. Therefore, abnormalities in IGF-1 signaling may explain the impaired cell proliferation and decreased bone formation that occurs in human osteoporosis.

In summary, the present study had for the first time demonstrated that UA confers a cytoprotective effect against glucocorticoids-induced cytotoxicity, oxidative stress and inflammation through induction of IGF-1-activated proliferation, antioxidant and anti-inflammation processes in MC3T3-E1 cells. Our study provides new insights into the role of UA in attenuating glucocorticoids-induced osteoporosis and a novel therapeutic strategy for osteoporosis.

## Acknowledgements

This study was supported by the Lishui Science and Technology program foundation of China (2014GYX006).

## Disclosure of conflict of interest

None.

**Address correspondence to:** Ye Zhu, Department of Orthopedics, 5th Affiliated Hospital, Lishui Central Hospital, Wenzhou Medical University, No 289 Kuocang Road, Lishui 323000, China. Tel: +86-0578-2285211; Fax: +86-0578-2285211; E-mail: zhuye1978@163.com

## References

[1] Cusano NE, Bilezikian JP. Combination anabolic and antiresorptive therapy for osteoporosis. Endocrinol Metab Clin North Am 2012; 41: 643-654.

[2] Hurson CJ, Butler JS, Keating DT, Murray DW, Sadlier DM, O'Byrne JM, Doran PP. Gene expression analysis in human osteoblasts exposed to dexamethasone identifies altered developmental pathways as putative drivers of osteoporosis. BMC Musculoskelet Disord 2007; 8: 12.

[3] Walsh S, Jordan G, Jefferiss C, Stewart K, Beresford J. High concentrations of dexamethasone suppress the proliferation but not the differentiation or further maturation of human osteoblast precursors in vitro: relevance to glucocorticoid-induced osteoporosis. Rheumatology 2001; 40: 74-83.

[4] McLaughlin F, Mackintosh J, Hayes B, McLaren A, Uings I, Salmon P, Humphreys J, Meldrum E, Farrow S. Glucocorticoid-induced osteopenia in the mouse as assessed by histomorphometry, microcomputed tomography, and biochemical markers. Bone 2002; 30: 924-930.

[5] Alm JJ, Heino TJ, Hentunen TA, Väänänen HK, Aro HT. Transient 100 nM dexamethasone treatment reduces inter-and intraindividual variations in osteoblastic differentiation of bone marrow-derived human mesenchymal stem cells. Tissue Eng Part C Methods 2012; 18: 658-666.

[6] Li H, Rajendran GK, Liu N, Ware C, Rubin BP, Gu Y. SirT1 modulates the estrogen-insulin-like growth factor-1 signaling for postnatal development of mammary gland in mice. Breast Cancer Res 2007; 9: R1.

[7] Feng Z, Levine AJ. The regulation of energy metabolism and the IGF-1/mTOR pathways by the p53 protein. Trends Cell Biol 2010; 20: 427-434.

[8] Rosen CJ. Insulin-like growth factor I and bone mineral density: experience from animal models and human observational studies. Best Pract Res Clin Endocrinol Metab 2004; 18: 423-435.

[9] Tanaka H, Quarto R, Williams S, Barnes J, Liang C. In vivo and in vitro effects of insulin-like growth factor-I (IGF-I) on femoral mRNA expression in old rats. Bone 1994; 15: 647-653.

[10] Perrini S, Carreira M, Conserva A, Laviola L, Giorgino F. Metabolic implications of growth hormone therapy. J Endocrinol Invest 2008; 31: 79-84.

[11] Perrini S, Natalicchio A, Laviola L, Cignarelli A, Melchiorre M, De Stefano F, Caccioppoli C, Leonardini A, Martemucci S, Belsanti G. Abnormalities of insulin-like growth factor-I signaling and impaired cell proliferation in osteoblasts from subjects with osteoporosis. Endocrinology 2008; 149: 1302-1313.

[12] Ovesna Z, Vachalkova A, Horvathova K, Tothova D. Pentacyclic triterpenoic acids: new chemoprotective compounds Minireview. Neoplasma 2004; 51: 327-333.
[13] Checker R, Sandur SK, Sharma D, Patwardhan RS, Jayakumar S, Kohli V, Sethi G, Aggarwal BB, Sainis KB. Potent anti-inflammatory activity of ursolic acid, a triterpenoid antioxidant, is mediated through suppression of NF-κB, AP-1 and NF-AT. PLoS One 2012; 7: e31318.
[14] Ikeda Y, Murakami A, Ohigashi H. Ursolic acid: An anti-and pro-inflammatory triterpenoid. Mol Nutr Food Res 2008; 52: 26-42.
[15] Tsai SJ, Yin MC. Antioxidative and anti-inflammatory protection of oleanolic acid and ursolic acid in pc12 cells. J Food Sci 2008; 73: H174-H178.
[16] Shishodia S, Majumdar S, Banerjee S, Aggarwal BB. Ursolic acid inhibits nuclear factor-κB activation induced by carcinogenic agents through suppression of IκBα kinase and p65 phosphorylation correlation with down-regulation of cyclooxygenase 2, matrix metalloproteinase 9, and cyclin D1. Cancer Res 2003; 63: 4375-4383.
[17] Lee SU, Park SJ, Kwak HB, Oh J, Min YK, Kim SH. Anabolic activity of ursolic acid in bone: Stimulating osteoblast differentiation in vitro and inducing new bone formation in vivo. Pharmacol Res 2008; 58: 290-296.
[18] Zhu FB, Wang JY, Zhang YL, Quan RF, Yue ZS, Zeng LR, Zheng WJ, Hou Q, Yan SG, Hu YG. Curculigoside regulates proliferation, differentiation, and pro-inflammatory cytokines levels in dexamethasone-induced rat calvarial osteoblasts. Int J Clin Exp Med 2015; 8: 12337.
[19] Liu YF, Qu GQ, Lu YM, Kong WM, Liu Y, Chen WX, Liao XH. Silencing of MAP4K4 by short hairpin RNA suppresses proliferation, induces G1 cell cycle arrest and induces apoptosis in gastric cancer cells. Mol Med Rep 2016; 13: 41-48.
[20] Owen TA, Aronow M, Shalhoub V, Barone LM, Wilming L, Tassinari MS, Kennedy MB, Pockwinse S, Lian JB, Stein GS. Progressive development of the rat osteoblast phenotype in vitro: reciprocal relationships in expression of genes associated with osteoblast proliferation and differentiation during formation of the bone extracellular matrix. J Cell Physiol 1990; 143: 420-430.
[21] Bradford MM. A rapid and sensitive method for the quantitation of microgram quantities of protein utilizing the principle of protein-dye binding. Anal Biochem 1976; 72: 248-254.
[22] Sun M, Xia R, Jin F, Xu T, Liu Z, De W, Liu X. Downregulated long noncoding RNA MEG3 is associated with poor prognosis and promotes cell proliferation in gastric cancer. Tumor Biol 2014; 35: 1065-1073.
[23] Rhen T, Cidlowski JA. Antiinflammatory action of glucocorticoids-new mechanisms for old drugs. N Engl J Med 2005; 353: 1711-1723.
[24] Spreafico A, Frediani B, Capperucci C, Leonini A, Gambera D, Ferrata P, Rosini S, Di Stefano A, Galeazzi M, Marcolongo R. Osteogenic growth peptide effects on primary human osteoblast cultures: Potential relevance for the treatment of glucocorticoid-induced osteoporosis. J Cell Biochem 2006; 98: 1007-1020.
[25] Lu J, Quearry B, Harada H. p38-MAP kinase activation followed by BIM induction is essential for glucocorticoid-induced apoptosis in lymphoblastic leukemia cells. FEBS Lett 2006; 580: 3539-3544.
[26] Yun SI, Yoon HY, Jeong SY, Chung YS. Glucocorticoid induces apoptosis of osteoblast cells through the activation of glycogen synthase kinase 3β. J Bone Miner Metab 2009; 27: 140-148.
[27] Ovesná Z, Kozics K, Slameňová D. Protective effects of ursolic acid and oleanolic acid in leukemic cells. Mutat Res 2006; 600: 131-137.
[28] Ramachandran S, Prasad NR. Effect of ursolic acid, a triterpenoid antioxidant, on ultraviolet-B radiation-induced cytotoxicity, lipid peroxidation and DNA damage in human lymphocytes. Chem Biol Interact 2008; 176: 99-107.
[29] Saravanan R, Pugalendi V. Impact of ursolic acid on chronic ethanol-induced oxidative stress in the rat heart. Pharmacol Rep 2006; 58: 41.
[30] Lu J, Zheng YL, Wu DM, Luo L, Sun DX, Shan Q. Ursolic acid ameliorates cognition deficits and attenuates oxidative damage in the brain of senescent mice induced by D-galactose. Biochem Pharmacol 2007; 74: 1078-1090.
[31] Kudo O, Sabokbar A, Pocock A, Itonaga I, Fujikawa Y, Athanasou N. Interleukin-6 and interleukin-11 support human osteoclast formation by a RANKL-independent mechanism. Bone 2003; 32: 1-7.
[32] Kanbur NÖ, Derman O, Kınık E. The relationships between pubertal development, IGF-1 axis, and bone formation in healthy adolescents. J Bone Miner Metab 2005; 23: 76-83.
[33] Muñoz-Torres M, Mezquita-Raya P, Lopez-Rodriguez F, Torres-Vela E, de Dios Luna J, Escobar-Jimenez F. The contribution of IGF-I to skeletal integrity in postmenopausal women. Clin Endocrinol 2001; 55: 759-766.
[34] Lacativa PG, Farias ML. Osteoporosis and inflammation. Arq Bras Endocrinol Metabol 2010; 54: 123-132.
[35] Wen B, Deutsch E, Marangoni E, Frascona V, Maggiorella L, Abdulkarim B, Chavaudra N, Bourhis J. Tyrphostin AG 1024 modulates radiosensitivity in human breast cancer cells. Br J Cancer 2001; 85: 2017.